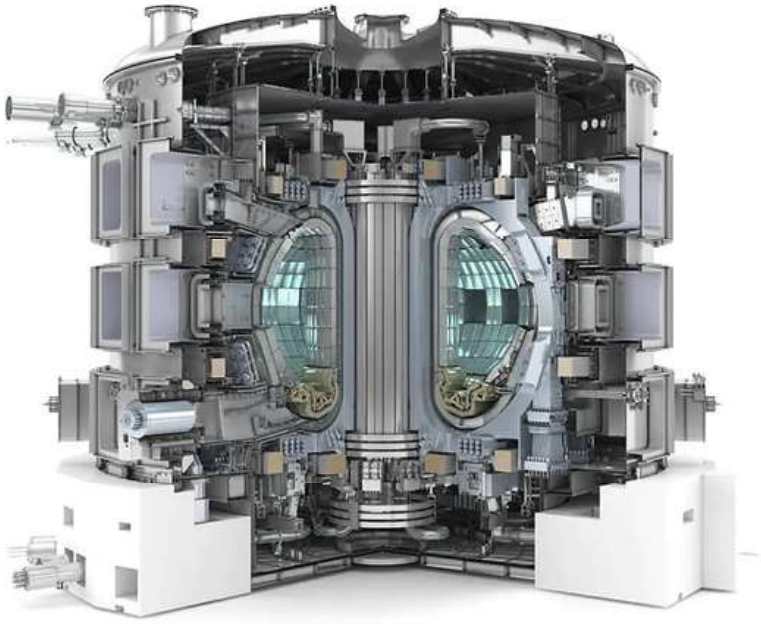
รายงานผลสัมฤทธิ์ภายใต้โครงการ

ITER RESEARCHER EXCHANGE PROGRAM 2025

หัวข้อ

TESTING FOR IN-VESSEL COIL POWER SUPPLY SYSTEM





นายพีรพัฒน์ ลิ่มบุญพา

การไฟฟ้าฝ่ายผลิตแห่งประเทศ

1 เมษายน – 31 พฤษภาคม 2569

ITER Organization

ประเทศฝรั่งเศส

FINAL REPORT

Visiting Researcher Programme at ITER Organization

Testing for In-vessel Coil Power Supply System (ICPS)

Prepared by:
Peeraphat Limbunpha — Visiting Researcher, EGAT
Host Organisation: ITER Organization — Power Electronics / ICPS team
Research Visit Period: 1 April – 29 May 2026
ITER Organization, Saint-Paul-lez-Durance, France

Table of Contents

1. Purpose 6
2. Scope 7
3. Abbreviations 8
4. Overview of ITER 9
   4.1 What is ITER? 9
   4.2 What is a Tokamak? 11
      4.2.1 Magnetic Confinement 12
      4.2.2 Plasma Heating 13
   4.3 ITER Key Systems 13
      4.3.1 Magnet System 13
      4.3.1.1 Toroidal Field (TF) Coils 14
      4.3.1.2 Poloidal Field (PF) Coils 15
      4.3.1.3 Central Solenoid (CS) 15
      4.3.1.4 Correction Coils 16
      4.3.1.5 Magnet Feeders 17
      4.3.2 Vacuum Vessel and In-Vessel Coils (IVC) 17
      4.3.2.1 Vacuum Vessel 17
      4.3.2.2 In-Vessel Coils (IVC) 18
5. In-Vessel Coil Power Supply System 20
   5.1 System Overview and ELM Architecture 20
   5.2 Power Electronics Assembly (PEA) 20
      5.2.1 PEA Cabinet Architecture 20
      5.2.2 Control System 25
   5.3 Site Acceptance Test (SAT) 26
      5.3.1 Delivery and Mechanical Inspection 27
      5.3.2 Cable Interconnection 27
      5.3.3 First Power-Up 28
      5.3.4 No-Load Test 28
      5.3.5 Light Load Test 29
      5.3.6 Normal Operation Test — 1-Hour Run 29
      5.3.7 Thermovision Monitoring 30
6. Current Sensor SMF Compatibility Test 32
   6.1 Background and Motivation 32
   6.2 Test Setup and Methodology 32
      6.2.1 Sensor Under Test 32
      6.2.2 Test Configurations 32
      6.2.3 Test Results 32
      6.2.3.1 Test T1 — Cable Installed + 100 A Injected 33
      6.2.3.2 Test T2 — Cable Installed, No Current 34
      6.2.3.3 Test T3 — No Cable, Standard Orientation 35
      6.2.3.4 Test T4 — No Cable, Sensor Rotated 90° 36
   6.3 Conclusions from SMF Test 37
7. Conclusions 39
8. Professional Development 40
9. References 41

List of Tables

Table 4.1 — Key Parameters of the ITER Tokamak. Source: ITER Organization (iter.org) 11
Table 4.2 — Key parameters of the ITER In-Vessel Coil (IVC) system. Source: ITER Organization ICPS documentation. 19
Table 5.1 — SAT test sequence summary: all seven phases PASS 31
Table 6.1 — SMF test summary: tested Hall-effect sensor disqualified for SMF Test (±10 A criterion) 37

List of Figures

Figure 4.1 — Computer-generated cutaway view of the ITER Tokamak Complex. Source: ITER Organization (iter.org) 9
Figure 4.2 — ITER Member Countries and their shares of the project. Source: ITER Organization (iter.org) 10
Figure 4.3 — Cross-section diagram of the ITER Tokamak showing major components. Source: ITER Organization (iter.org) 11
Figure 4.4 — Overview of the ITER superconducting magnet system. Source: ITER Organization (iter.org/machine/magnets) 14
Figure 4.5 — ITER Toroidal Field Coils: 18 D-shaped superconducting coils arranged around the vacuum vessel. Source: ITER Organization (iter.org/machine/magnets) 14
Figure 4.6 — ITER Poloidal Field Coils: 6 ring-shaped superconducting coils positioned around the outer structure. Source: ITER Organization (iter.org/machine/magnets) 15
Figure 4.7 — ITER Central Solenoid: six stacked coil modules. Source: ITER Organization (iter.org/machine/magnets) 16
Figure 4.8 — ITER Correction Coils: 18 coils positioned between TF and PF coil structures. Source: ITER Organization (iter.org/machine/magnets) 16
Figure 4.9 — The ITER Vacuum Vessel: a double-walled steel torus, 19.4 m outer diameter, 11.4 m height. Source: ITER Organization (iter.org/machine/vacuum-vessel) 18
Figure 4.10 — In-Vessel Coils (IVC): ELM control coils (27 coils on vessel wall) and vertical stability coils (above and below mid-plane). Source: ITER Organization (iter.org/machine/magnets) 19
Figure 5.1 — PEA complete connection diagram 21
Figure 5.2 — Line Filter & Control Cabinet photo 21
Figure 5.3 — Transformer Cabinet photo 22
Figure 5.4 — Thyristor Rectifier Cabinet photo 22
Figure 5.5 — DC Link Cabinet photo 23
Figure 5.6 — FOCS Cabinet 24
Figure 5.7 — IGBT Inverter Cabinet photo 24
Figure 5.8 — Load Cabinet photo (bottom) 25
Figure 5.9 — Real-time controller in the line filter and control cabinet during SAT. The HMI connects via Ethernet; the FPGA board handles time-critical gate drive and I/O at hardware speed. 26
Figure 5.10 — Electrical safety practice at the ITER site: PPE and safety briefing before SAT activities 26
Figure 5.11 — PEA cabinets transported to the SAT test area at the ITER site, 29 April 2026 27
Figure 5.12 — Cabinet positioned and ready for mechanical inspection at the ITER SAT area 27
Figure 5.13 — Cable interconnection activities (1–3 May 2026): power busbar routing and signal harness installation between cabinets 28
Figure 5.14 — First power-up (4 May 2026): HMI active and control system communicating after initial energisation 28
Figure 5.15 — No-Load Test: oscilloscope captures of IGBT gate-drive waveforms confirming gate-drive levels, deadtime, and absence of shoot-through events 29
Figure 5.16 — Light Load Test: test activity (left) and output current waveform (right) confirming stable closed-loop current tracking at reduced setpoint 29
Figure 5.17 — Normal Operation Test: 1-hour rated current waveform trace (left) and test team monitoring the system (right). Both current and DC-link voltage remain stable throughout. 30
Figure 5.18 — Thermovision: IR scans of IGBT heatsinks (left) confirming uniform heat distribution; temperature/FOCS monitoring (right) 30
Figure 6.1 — Pre-test baseline: sensor output at rated 1000 A with no applied SMF, all four configurations within ±1 A (reference). 33
Figure 6.2 — T1: Test setup — primary cable (~100 A RMS AC) routed through the sensor aperture. 33

Figure 6.3 — T1: Calculated current (green, left axis) vs. B-field (right axis). Output tracks SMF steps rather than the 100 A primary current. 34
Figure 6.4 — T2: Test setup — cable still installed in the sensor aperture with no current injected (same physical configuration as T1). 34
Figure 6.5 — T2: With no current injected, the sensor output mirrors the B-field steps identically. 35
Figure 6.6 — T3: Test setup — sensor with the primary cable removed, standard orientation. 35
Figure 6.7 — T3: Even without a cable, calculated current closely tracks the B-field — confirming intrinsic sensor susceptibility. 36
Figure 6.8 — T4: Test setup — sensor with cable removed, rotated 90° relative to the dominant field direction. 36
Figure 6.9 — T4: Rotated 90° — error reduces to ~−13 to −16 A but remains outside specification. Note high noise at field step transitions. 37

1. Purpose

This report documents the activities, findings, and technical insights gained during the visiting researcher programme at the ITER Organization, carried out from 1 April to 29 May 2026 in Saint-Paul-lez-Durance, southern France. The programme was arranged under the Cooperation Agreement between the Thailand Institute of Nuclear Technology (TINT) and the ITER Organization.

The primary purpose of this report is to present a comprehensive account of participation in the In-Vessel Coil Power Supply (ICPS) project at ITER, including technical background study, review of Factory Acceptance Test (FAT) documentation, and hands-on participation in the Site Acceptance Testing (SAT) of the Power Electronics Assembly (PEA) prototype. The report is intended to serve as a reference document for engineers and management who may seek to leverage knowledge gained from ITER activities in the context of Thailand's future energy strategy and nuclear technology development.

Specific objectives of this report include:

- To provide an overview of the ITER project, its scientific goals, and its key engineering systems.
- To describe the technical scope and design of the In-Vessel Coil Power Supply (ICPS) system.
- To document the test procedures and results related to the Power Electronics Assembly (PEA) Factory Acceptance Testing.

The report is organised as follows: Sections 1 through 4 present the purpose, scope, and a general overview of the ITER project and its key machine systems; Section 5 details the ICPS technical work, including the PEA architecture and Site Acceptance Testing; Section 6 documents the static magnetic field (SMF) compatibility testing of a commercial Hall-effect current sensor; and Sections 7 and 8 present the overall conclusions and professional development outcomes of the visit.

2. Scope

This report covers the technical and scientific activities conducted during the two-month visiting researcher period at ITER. The scope encompasses the following areas:

1. General Overview of ITER: Background of the project, scientific objectives, international collaboration structure, and key machine systems including the tokamak, magnet systems, vacuum vessel, and in-vessel components.
2. In-Vessel Coil Power Supply (ICPS) System: System architecture, functional specifications, and design documentation review. This includes study of the ELM (Edge-Localised Mode) coil power supply and the Vertical Stability (VS) coil power supply sub-systems.
3. Power Electronics Assembly (PEA) Acceptance Testing: Review of the Factory Acceptance Test (FAT) documentation and participation in the Site Acceptance Test (SAT) of the IVC PEA prototype, including cable interconnection, first power-up, no-load, light-load, rated-current operation, and thermovision monitoring.
4. Current Sensing and Measurement: Technical review of Hall-effect current sensors considered for use in the ICPS environment, including test procedures and conformance assessment.
5. Observations and Lessons Learned: Personal reflections on the engineering culture, advanced technology environment at ITER.

3. Abbreviations

The following abbreviations are used throughout this report:

Abbreviation	Definition
AC	Alternating Current
CPS	Coil Power Supply
CS	Central Solenoid
D-T	Deuterium-Tritium
DA	Domestic Agency
DC	Direct Current
EGAT	Electricity Generating Authority of Thailand
ELM	Edge-Localized Mode
EMF	Electromotive Force
FAT	Factory Acceptance Testing
GJ	Gigajoule
HTS	High-Temperature Superconductor
ICPS	In-Vessel Coil Power Supply
IGBT	Insulated Gate Bipolar Transistor
IO	ITER Organization
IVC	In-Vessel Coil(s)
ITER	International Thermonuclear Experimental Reactor
kA	Kiloampere
MA	Megaampere
MW	Megawatt
Nb-Ti	Niobium-Titanium (superconductor material)
Nb3Sn	Niobium-Tin (superconductor material)
PEA	Power Electronics Assembly
PF	Poloidal Field
Q	Energy Gain Factor (fusion power / input power)
QA	Quality Assurance
SMF	Static Magnetic Field
TF	Toroidal Field
TINT	Thailand Institute of Nuclear Technology
VV	Vacuum Vessel
VS	Vertical Stability

4. Overview of ITER

4.1 What is ITER?

ITER — meaning "The Way" in Latin and standing for International Thermonuclear Experimental Reactor — is one of the most ambitious and technically complex scientific endeavours in human history. It is a massive experimental fusion device being constructed in Saint-Paul-lez-Durance, in the Provence region of southern France. The machine is designed to demonstrate, for the first time, that nuclear fusion can be harnessed as a large-scale, carbon-free source of energy.

The concept for ITER originated at the 1985 Geneva Superpower Summit between US President Ronald Reagan and Soviet General Secretary Mikhail Gorbachev, who called for an international effort to develop fusion energy for peaceful purposes. The ITER Agreement was formally signed in 2006, and construction of the ITER site began in 2010. As of 2026, the project is progressing through the machine assembly phase at its 42-hectare site.

ITER is not a power plant. Its primary purpose is scientific and technological: to demonstrate that fusion can produce more energy than it consumes, to test integrated fusion technologies at reactor scale, and to pave the way for a commercial fusion demonstration plant (DEMO) in the second half of this century. The machine is specifically designed to:

- Achieve a deuterium-tritium plasma in which fusion self-heating dominates, a condition known as "burning plasma."
- Generate 500 MW of fusion power from only 50 MW of input heating power — a tenfold energy gain (Q = 10).
- Test key technologies required for fusion power plants, such as superconducting magnets, remote maintenance systems, tritium breeding, and plasma control.
- Demonstrate the safety characteristics and environmental compatibility of a fusion device.

For context: the previous fusion power record, set by the European tokamak JET in 1997, achieved Q ≈ 0.67. ITER targets Q = 10 — a qualitative leap in fusion performance.

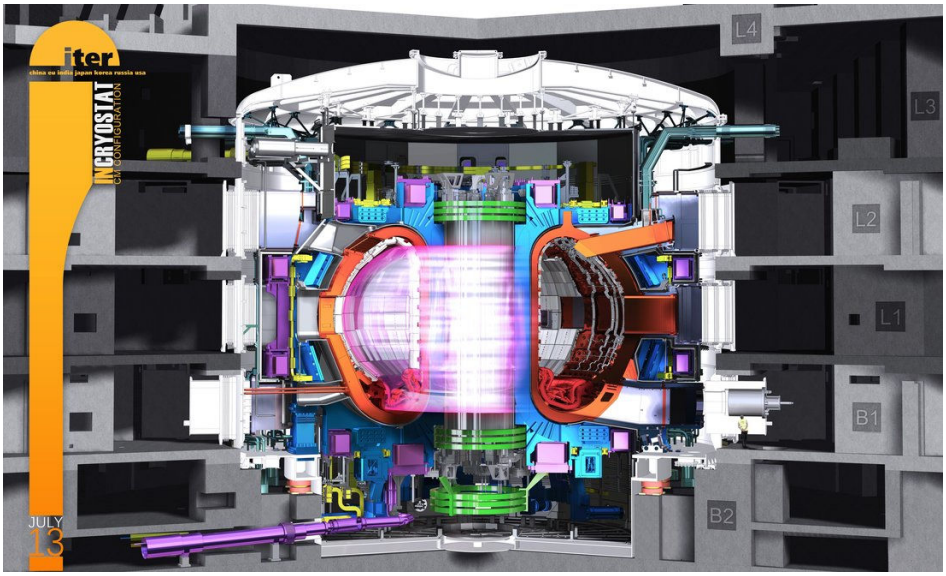


Figure 4.1 — Computer-generated cutaway view of the ITER Tokamak Complex. Source: ITER Organization (iter.org)

The ITER project is the product of a uniquely broad international collaboration. Seven Members — China, the European Union (through Euratom), India, Japan, Korea, Russia, and the United States — have joined resources to build and operate ITER. Collectively, these Members represent three continents, over 40 languages, more than half of the world's population, and approximately 73% of global GDP. Thailand, through TINT, holds a Cooperation Agreement with the ITER Organization, allowing Thai researchers to engage with the project.

Construction costs are shared among the seven Members, with Europe contributing the largest share. Crucially, nine-tenths of all contributions are made in-kind — as fabricated components, systems, or buildings — driving a global wave of advanced manufacturing tied to the project.

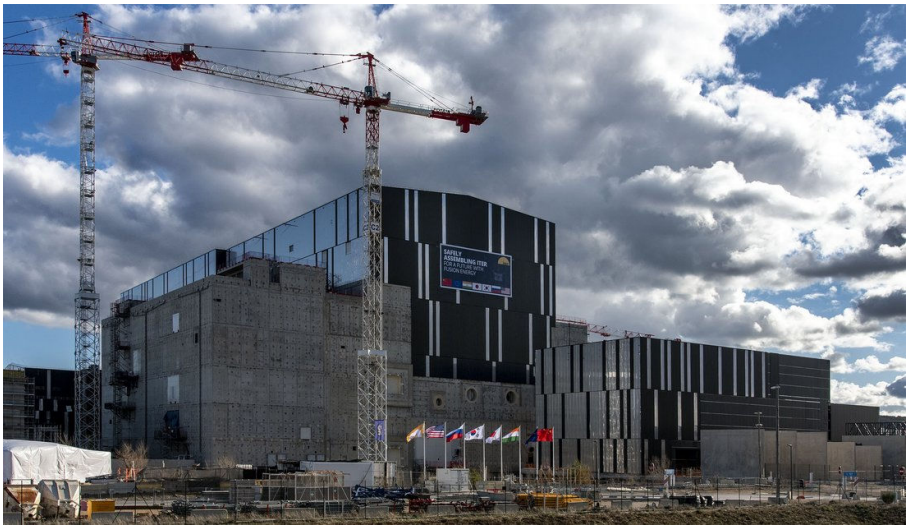


Figure 4.2 — ITER Member Countries and their shares of the project. Source: ITER Organization (iter.org)

ITER will be the world's largest tokamak: twice the linear dimensions of the largest currently operating machine (JT-60SA in Japan) and with six times its plasma chamber volume. Assembly of the machine began in 2020, and under the updated 2024 baseline, the Start of Research Operation is projected for 2034, with deuterium-tritium operation beginning in 2039.

Table 4.1 below summarises the key parameters of ITER:

Parameter	Value
Total Fusion Power Output	**500 MW**
Energy Gain Factor (Q)	**≥ 10**
Plasma Volume	**840 m³**
Vacuum Vessel Interior Volume	**1,400 m³**
Plasma Current	**15 MA**
Toroidal Magnetic Field	**5.3 Tesla at plasma axis**
Plasma Pulse Duration	**300–500 seconds**
Total Machine Height (with cryostat)	**~29 m**
Total Machine Weight	**~23,000 tonnes**

Parameter	Value
Magnet System Stored Energy	**51 GJ**
Number of Main TF Coils	**18**
Plasma Temperature (operational)	**~150,000,000 °C**
Site Area	**42 hectares**
Start of Research Operation (projected)	**2034**
Start of D-T Operation (projected)	**2039**

Table 4.1 — Key Parameters of the ITER Tokamak. Source: ITER Organization (iter.org)

4.2 What is a Tokamak?

A tokamak is an experimental device designed to confine and heat a plasma to the extreme temperatures required for nuclear fusion to occur. The word "tokamak" derives from a Russian acronym — тороидальная камера с магнитными катушками — meaning "toroidal chamber with magnetic coils." The concept was first developed by Soviet physicists Igor Tamm and Andrei Sakharov in the late 1950s, and since then the tokamak has emerged as the world's most promising configuration for a magnetic fusion reactor.

The heart of a tokamak is its doughnut-shaped (toroidal) vacuum chamber. Inside this chamber, under the combined influence of extreme heat and powerful magnetic fields, gaseous hydrogen fuel is ionised into a plasma — often described as the fourth state of matter. At plasma temperatures of 150 million degrees Celsius (ten times hotter than the core of the Sun), hydrogen isotopes (deuterium and tritium) collide with enough energy to overcome their natural electromagnetic repulsion and fuse together, releasing enormous amounts of energy in the process.

ITER's fusion reaction combines a deuterium nucleus with a tritium nucleus to produce a helium-4 nucleus (alpha particle) and a high-energy neutron, releasing about 17.6 MeV of energy per reaction. Most of this energy is carried away by the neutron, while the helium nucleus deposits its share back into the plasma, sustaining a self-heating “burning plasma” — the primary scientific objective of ITER.

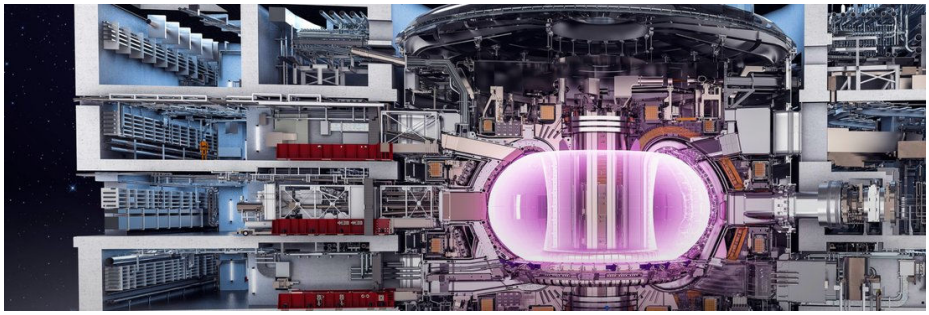


Figure 4.3 — Cross-section diagram of the ITER Tokamak showing major components. Source: ITER Organization (iter.org)

Unlike conventional power plants that rely on chemical combustion or nuclear fission, a tokamak generates energy through nuclear fusion — releasing vastly more energy per unit mass than either, while producing no greenhouse gases, no long-lived radioactive waste, and no risk of a runaway chain reaction.

A fusion power plant based on the tokamak concept would work as follows: the neutrons released from the D-T fusion reaction would be absorbed by the surrounding walls and

blanket of the reactor, where their kinetic energy would be converted to heat. This heat would then drive a steam turbine-generator cycle, producing electricity — exactly as in a conventional thermal power plant. From an electrical engineering perspective, a fusion power plant would connect to the grid in the same manner as any other synchronous generator-based power plant.

Three conditions must simultaneously be met to achieve a self-sustaining fusion reaction in a laboratory setting, collectively described by the Lawson Criterion:

- Sufficient Temperature: The plasma must reach approximately 150 million °C (about ten times the temperature at the Sun's core). At this temperature, the thermal energy of the nuclei is sufficient to overcome their electrostatic repulsion and allow fusion to occur.
- Sufficient Plasma Density: The plasma must be dense enough that collisions between fuel nuclei occur frequently enough to sustain a useful reaction rate.
- Sufficient Confinement Time: The plasma must be held together long enough — at sufficient temperature and density — for the energy released by fusion to exceed the energy required to heat and maintain the plasma.

ITER's tokamak is designed to satisfy all three conditions simultaneously at power-plant-relevant scale.

4.2.1 Magnetic Confinement

At 150 million degrees Celsius, no material can physically contain a plasma. The solution, first conceived in the 1950s, is to use powerful magnetic fields to confine the plasma away from the vessel walls. A charged particle moving through a magnetic field experiences a force perpendicular to both its direction of motion and the field direction (the Lorentz force), causing it to spiral along the magnetic field lines rather than travel in a straight line.

In a tokamak, the magnetic confinement is achieved through the superposition of two magnetic field components:

- Toroidal Field (TF): A strong magnetic field running around the circumference of the torus (the "long way around"), generated by the toroidal field coils surrounding the vacuum vessel. This is the dominant confining field.
- Poloidal Field (PF): A field component running around the cross-section of the torus (the "short way around"), generated by a combination of the plasma current itself and the poloidal field coils. The poloidal field is essential for plasma shaping, stability, and positioning.

The combination of these two field components creates a helical magnetic field configuration. Plasma particles spiral along these helical field lines and, in an ideal torus, never touch the vessel walls. This is the fundamental principle of tokamak confinement.

In practice, perfect confinement is never achieved. Turbulence, instabilities, and geometric effects all cause some plasma particles to drift toward the vessel walls. Controlling these effects — through precise magnetic field shaping, active feedback control, and sophisticated plasma physics — is one of the central technical challenges of fusion research. ITER's design incorporates multiple coil systems and advanced control algorithms specifically to manage these phenomena.

The quality of magnetic confinement is described by the energy confinement time — a measure of how long the plasma retains its thermal energy. ITER is designed to achieve a

confinement time sufficient, combined with its plasma temperature and density, to satisfy the Lawson Criterion and reach burning-plasma conditions.

4.2.2 Plasma Heating

While the plasma in ITER will ultimately be sustained by the self-heating from the alpha particles produced in the fusion reaction, external heating is required to bring the plasma to fusion temperature in the first place. ITER uses three complementary heating systems, which together provide 50 MW of auxiliary heating power:

- Ohmic Heating: The changing magnetic flux driven by the central solenoid induces a plasma current, which heats the plasma resistively — much like current flowing through a resistor. This effect is strongest at lower temperatures and weakens as the plasma heats up.
- Neutral Beam Injection (NBI): High-energy beams of neutral hydrogen atoms are injected directly into the plasma. Because the atoms are neutral, they pass through the magnetic field and penetrate deep into the plasma before being ionised by collisions and transferring their energy to it.
- Radiofrequency (RF) Heating: Electromagnetic waves are launched into the plasma at frequencies tuned to the natural resonance of electrons (Electron Cyclotron Resonance Heating, ECRH) or ions (Ion Cyclotron Resonance Heating, ICRH), allowing the particles to absorb the wave energy very efficiently.

Once burning plasma is achieved, self-heating from alpha particles will vastly exceed the auxiliary heating input — the key transition from today's externally-heated experiments to a true fusion reactor.

4.3 ITER Key Systems

The ITER tokamak comprises around one million individual components and stands as one of the largest engineering structures ever built (see Table 4.1). The key systems are introduced below, with particular emphasis on the magnet system and vacuum vessel — the systems most directly relevant to the ICPS work conducted during this visiting researcher period.

The primary systems of the ITER tokamak can be grouped as follows:

- Magnet System (superconducting coils: TF, PF, CS, correction coils, and in-vessel coils)
- Vacuum Vessel (the plasma chamber and first confinement barrier)
- Blanket (neutron shielding and future tritium breeding)
- Divertor (exhaust of plasma impurities and heat)
- Cryostat (vacuum vessel enclosing the superconducting magnet system at cryogenic temperatures)
- Supporting Systems (heating systems, cryogenics, fuel cycle, diagnostics, remote handling, power supply, control)

4.3.1 Magnet System

The ITER magnet system is the largest and most technically complex integrated superconducting magnet system ever built, storing the enormous magnetic energy needed to initiate, confine, shape, and control the ITER plasma.

The magnets operate in the superconducting state, cooled to about 4 Kelvin using supercritical helium. At this temperature, the niobium-tin (Nb_3Sn) and niobium-titanium (Nb-Ti) conductors carry current with zero resistance, avoiding the enormous ohmic losses that conventional copper conductors would incur at these current levels.

The ITER conductors use an advanced "cable-in-conduit conductor" (CICC) design: superconducting strands are cabled together and enclosed in a structural steel jacket through which supercritical helium flows for cooling. Producing the required Nb_3Sn superconducting strand was itself a major global industrial achievement.

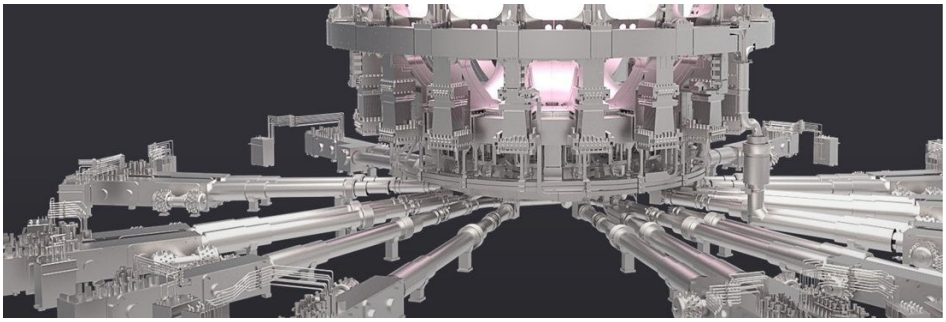


Figure 4.4 — Overview of the ITER superconducting magnet system. Source: ITER Organization (iter.org/machine/magnets)

The ITER magnet system consists of five distinct coil types, each with a specific role:

4.3.1.1 Toroidal Field (TF) Coils

The 18 “D”-shaped toroidal field (TF) coils are the primary plasma-confining magnets, generating the dominant toroidal field used to confine the plasma. Wound from Nb_3Sn superconductor and encased in stainless steel structural cases, they were jointly fabricated by Europe (Fusion for Energy) and Japan under a coordinated parallel fabrication programme.

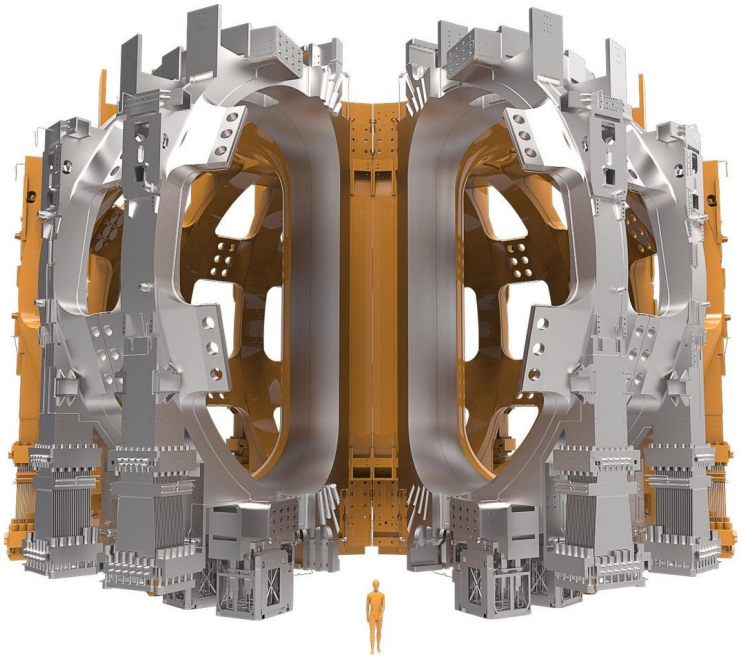


Figure 4.5 — ITER Toroidal Field Coils: 18 D-shaped superconducting coils arranged around the vacuum vessel. Source: ITER Organization (iter.org/machine/magnets)

4.3.1.2 Poloidal Field (PF) Coils

Six ring-shaped poloidal field (PF) coils, stacked along the machine's vertical axis, shape the plasma cross-section, contribute to plasma stability, and work with the central solenoid to control the plasma current profile and vertical position. Fabricated from the more flexible Nb-Ti superconductor, several of the largest coils were too large to transport by road and were wound directly on the ITER site.

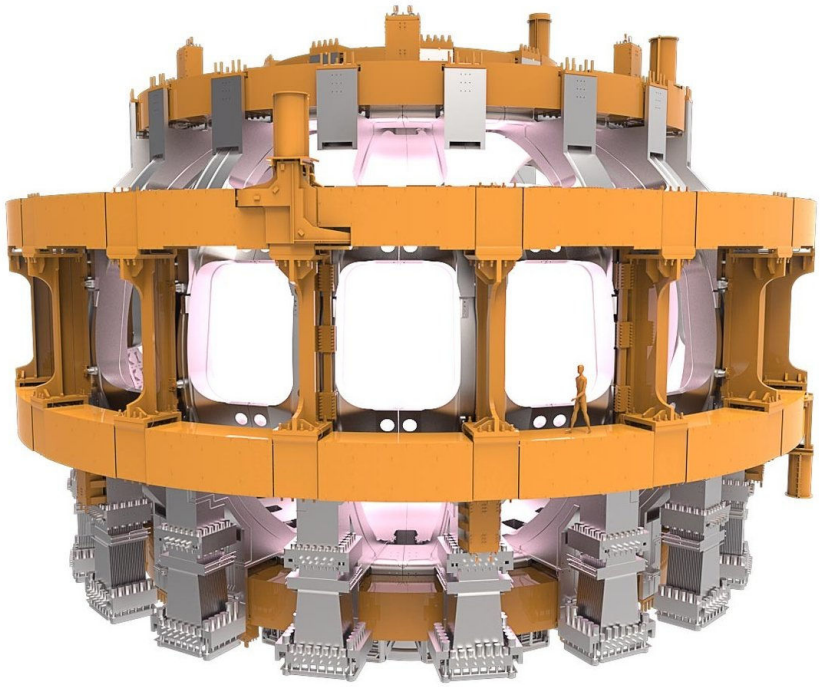


Figure 4.6 — ITER Poloidal Field Coils: 6 ring-shaped superconducting coils positioned around the outer structure. Source: ITER Organization (iter.org/machine/magnets)

4.3.1.3 Central Solenoid (CS)

The central solenoid (CS) is the "heart" of ITER's inductive plasma control system and the most powerful individual magnet in the machine — a tall stack of six independently operable coil modules. Acting as the primary winding of a transformer, it induces the plasma current essential for tokamak operation and contributes Ohmic heating. Wound from Nb_3Sn superconductor, the CS achieves the highest field of any ITER magnet and can drive long plasma pulses; it was manufactured by General Atomics (USA) and fully installed in the ITER machine by 2025.



Figure 4.7 — ITER Central Solenoid: six stacked coil modules. Source: ITER Organization (iter.org/machine/magnets)

4.3.1.4 Correction Coils

Eighteen superconducting correction coils, arranged in three groups of six around the machine, compensate for small magnetic field errors arising from manufacturing and assembly tolerances in the main coils — providing a final "trim" capability needed to preserve plasma confinement quality.

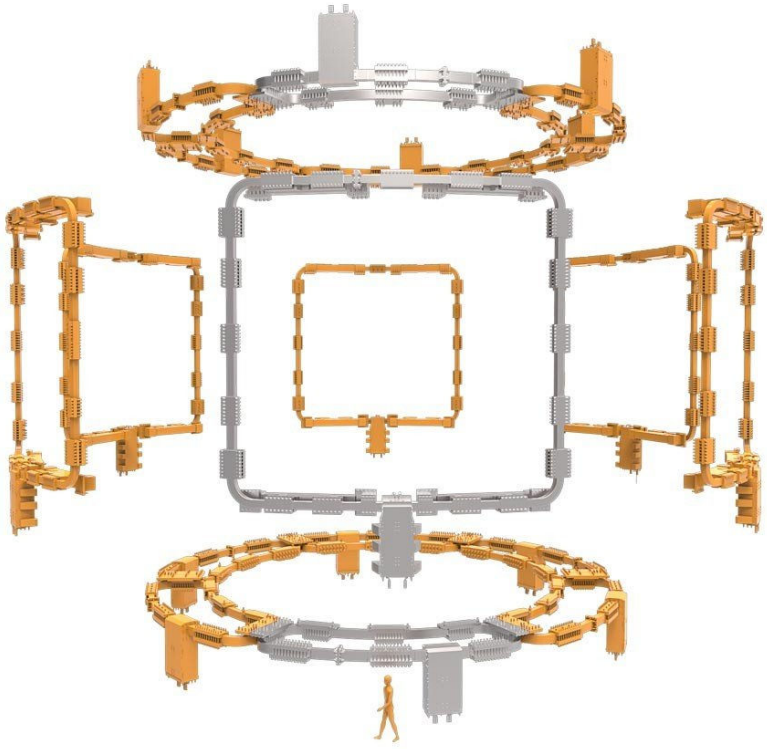


Figure 4.8 — ITER Correction Coils: 18 coils positioned between TF and PF coil structures. Source: ITER Organization (iter.org/machine/magnets)

4.3.1.5 Magnet Feeders

The 31 superconducting magnet feeders connect the room-temperature power supplies to the 4-Kelvin coils, each carrying both high electrical currents and the cryogenic liquids needed for cooling across the cryostat's warm-cold barrier. High-Temperature Superconductor (HTS) current leads minimise the heat conducted into the cold region — a critical requirement given how costly cryogenic refrigeration is per watt removed.

4.3.2 Vacuum Vessel and In-Vessel Coils (IVC)

4.3.2.1 Vacuum Vessel

The ITER vacuum vessel (VV) is a hermetically sealed, double-walled stainless steel container that encloses the plasma and provides the controlled environment in which fusion experiments take place. It is the first safety confinement barrier of the ITER machine, designed to contain the radioactive tritium fuel and any fusion products in the event of an accident.

The vacuum vessel serves multiple critical functions:

- Plasma Environment: The interior of the VV is maintained under high vacuum to provide the plasma-grade environment required for fusion, preventing contamination and energy loss.
- Safety Confinement: The VV acts as the primary confinement barrier for radioactivity (tritium and activation products). Its double-wall construction provides redundant containment, and cooling water circulates between the walls to remove heat generated during plasma operation.
- Neutron Shielding: The walls of the VV, combined with the blanket modules installed on the inner surface, provide shielding from the 14.1 MeV neutrons produced by the D-T fusion reaction, protecting the superconducting magnets from neutron-induced damage and nuclear heating.
- Structural Support: The VV provides the structural platform on which the blanket modules and divertor cassettes are mounted. It must withstand electromagnetic forces from the magnets, thermal stresses, and the mechanical loads from in-vessel components.
- Access for Systems: Multiple ports in the VV wall provide access for heating systems, diagnostics, fuelling, vacuum pumping, and remote maintenance operations.

The ITER vacuum vessel is a technically extraordinary structure — one of the largest and heaviest components of the machine, with an interior volume several times larger than that of any currently operating tokamak (see Table 4.1).

The VV is constructed as nine equal sectors, fabricated by ITER's Domestic Agencies and transported to the site, where they were integrated into sector modules together with the associated TF coils and thermal shields before being lowered into the tokamak pit for assembly.

Between the double walls of the VV, modular blocks of borated and ferromagnetic stainless steel ("in-wall shielding") provide additional neutron shielding and help control the toroidal field ripple effect.

Thermal shielding is installed between the VV and the cryostat to prevent heat radiating from the vacuum vessel from reaching the 4 K cryogenic environment of the superconducting magnets.

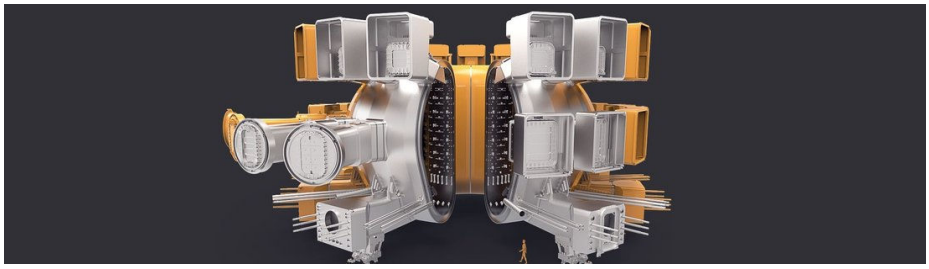


Figure 4.9 — The ITER Vacuum Vessel: a double-walled steel torus, 19.4 m outer diameter, 11.4 m height. Source: ITER Organization (iter.org/machine/vacuum-vessel)

4.3.2.2 In-Vessel Coils (IVC)

Inside the vacuum vessel, two non-superconducting coil systems provide additional plasma control capabilities that cannot be achieved by the main external superconducting coils. These are collectively called the In-Vessel Coils (IVC), and they are the subject of the ICPS system which was the primary focus of work during this visiting researcher period.

The IVC consists of two distinct coil systems:

- Vertical Stability (VS) Coils: Two coil assemblies installed above and below the machine's mid-plane, providing fast vertical stabilisation. Because ITER's elongated plasma column is inherently unstable against vertical displacements, the VS coils provide active feedback control to counteract these movements within milliseconds, preventing disruptive "vertical displacement events" (VDEs).
- ELM Control Coils: 27 coils (3 rows of 9) fixed to the inner wall of the vessel, generating resonant magnetic perturbations that suppress Edge-Localised Modes (ELMs) — periodic energy bursts from the plasma edge that would otherwise erode the divertor. This allows the plasma to operate in high-confinement mode (H-mode) while keeping divertor heat loads manageable.

Because the IVC are located inside the vacuum vessel — in the same environment as the plasma — they present unique engineering challenges not faced by the external superconducting coils:

- High Radiation Environment: The coils are exposed to intense neutron and gamma radiation from the plasma, which can cause radiation damage to conductor insulation and other materials over time.
- High Thermal Load: The coils must operate in the presence of significant heat from the plasma and from nuclear heating by neutrons.
- High Vacuum Compatibility: All materials used in the IVC must be compatible with the ultra-high vacuum environment and must not outgas contaminants that would degrade plasma performance.
- Electromagnetic Forces: Carrying large currents in the presence of the strong external magnetic field, the IVC are subjected to significant electromagnetic (Lorentz) forces, which must be accounted for in their structural design and mounting.

To address these challenges, the IVC are manufactured from a special type of mineral-insulated copper conductor (MICC). Unlike conventional magnet conductors that use

organic polymer insulation (which would be damaged by radiation and high temperatures), MICC uses a mineral — typically magnesium oxide (MgO) — as the insulating material. MgO is highly radiation-resistant, thermally stable, and vacuum-compatible, making it the material of choice for in-vessel electrical conductors in fusion machines.

The IVC are not superconducting, operating at room temperature and carrying modest currents relative to the main coils (see Table 4.2). Their key requirement is speed: the VS coils must respond to plasma position changes within milliseconds, while the ELM coils must apply precisely controlled, time-varying perturbation fields synchronised with the plasma edge.

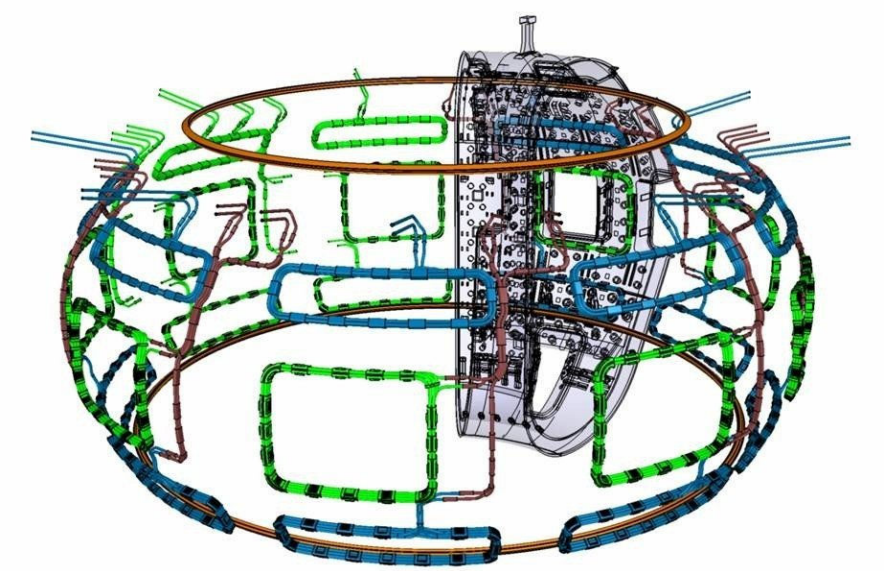


Figure 4.10 — In-Vessel Coils (IVC): ELM control coils (27 coils on vessel wall) and vertical stability coils (above and below mid-plane). Source: ITER Organization (iter.org/machine/magnets)

The power supply system for the In-Vessel Coils — the In-Vessel Coil Power Supply (ICPS) — must deliver these rapidly varying, precisely controlled currents to coils located inside the vacuum vessel through carefully designed feedthroughs that pass the warm-cold and vacuum barriers of the machine. The ICPS is the central subject of this report and is described in detail in subsequent sections.

Table 4.2 summarises the key parameters of the In-Vessel Coil system:

Parameter	VS Coils	ELM Coils	Unit
Number of coils	2 (top + bottom)	27 (3 × 9 rows)	—
Conductor type	Mineral-insulated copper	Mineral-insulated copper	—
Peak current	±52	±10	kA
Voltage to ground	±3.3	±3.3	kV
Primary function	Vertical stabilisation	ELM suppression/control	—
Response time	< 10	< 1 (ELM freq.)	ms
Operating temperature	Room / elevated	Room / elevated	°C

Table 4.2 — Key parameters of the ITER In-Vessel Coil (IVC) system. Source: ITER Organization ICPS documentation.

5. In-Vessel Coil Power Supply System

5.1 System Overview and ELM Architecture

The ITER In-Vessel Coil (IVC) system is installed directly on the inner wall of the vacuum vessel and operates in a uniquely challenging environment: extreme heat loads, intense neutron flux, and strong stray magnetic fields. Two subsystems serve distinct plasma control functions:

- ELM Control Coils: 27 coils in three toroidal rows (upper, middle, lower — 9 coils per row). They generate resonant magnetic perturbations (RMPs) to suppress Edge Localised Modes (ELMs) — periodic MHD instabilities that release damaging energy bursts onto the divertor.
- Vertical Stabilisation Coils (VS3): Two coil assemblies installed above and below the machine's mid-plane, providing fast vertical position control of the plasma, counteracting vertical displacement events (VDEs) on millisecond timescales.

Each of the 27 ELM coils requires its own dedicated two-stage power converter: a thyristor phase-controlled rectifier stage followed by an IGBT H-bridge PWM inverter stage, under real-time digital control. The strong stray magnetic field precludes conventional Hall-effect sensors, driving the adoption of Fibre Optic Current Sensor (FOCS) technology based on the Faraday magneto-optic effect.

5.2 Power Electronics Assembly (PEA)

The PEA is a full-function, reduced-scale prototype of the ELM coil power supply, built by an external industrial supplier under contract to the ITER Organization. It replicates the production design at a reduced current rating, validating the electronics, control algorithms, and protection responses before committing to series production of the 27 production units. The PEA underwent Factory Acceptance Testing (FAT) at the supplier's premises and Site Acceptance Testing (SAT) at the ITER site.

5.2.1 PEA Cabinet Architecture

Seven interconnected cabinets form the complete power conversion chain from three-phase AC input to controlled AC current output. Power flows from the line filter and control cabinet through the isolation transformer, thyristor rectifier, DC-link bank, and FOCS measurement cabinet, to the IGBT H-bridge inverter and finally the resistive-inductive load cabinet.

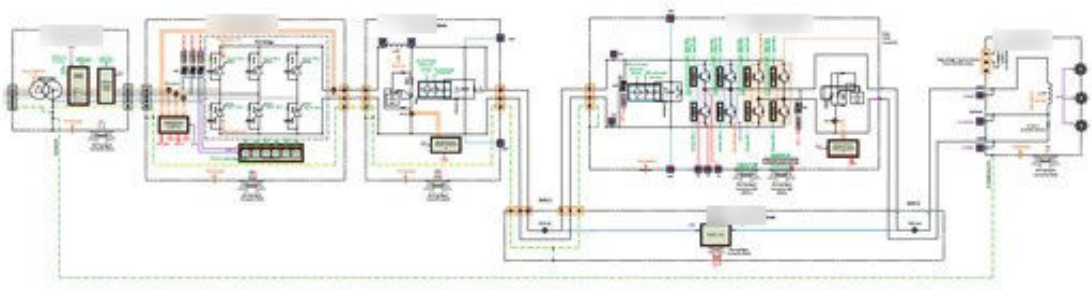


Figure 5.1 — PEA complete connection diagram

Line Filter & Control Cabinet — Houses the main protection, line filters, auxiliary power supplies, and the real-time controller and FPGA interface board that execute the complete closed-loop current control algorithm.



Figure 5.2 — Line Filter & Control Cabinet photo

Transformer Cabinet — Steps down the supply voltage and provides galvanic isolation between the utility grid and the converter power stages.



Figure 5.3 — Transformer Cabinet photo

Thyristor Rectifier Cabinet — A three-phase fully controlled thyristor bridge converts AC to DC; the controller adjusts the firing angle to set the DC-link voltage. Earth continuity and insulation resistance were confirmed in FAT.

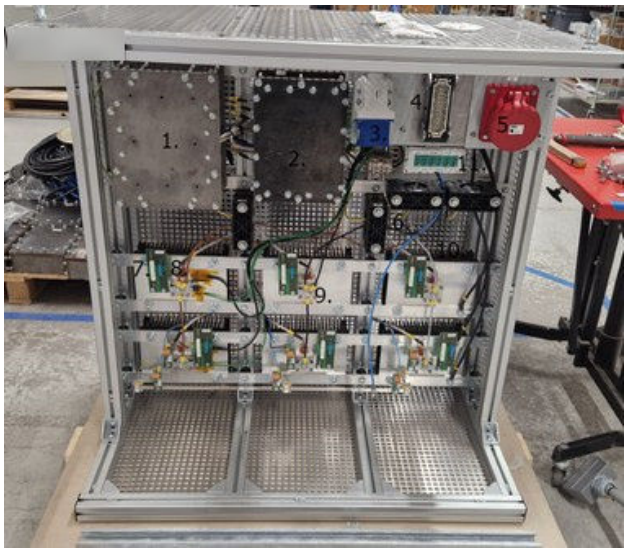


Figure 5.4 — Thyristor Rectifier Cabinet photo

DC Link Cabinet — A capacitor bank buffers energy, smooths ripple and provides an energy reserve for fast transients. A crowbar and discharge contactors ensure safe de-energisation after the supply is disconnected.

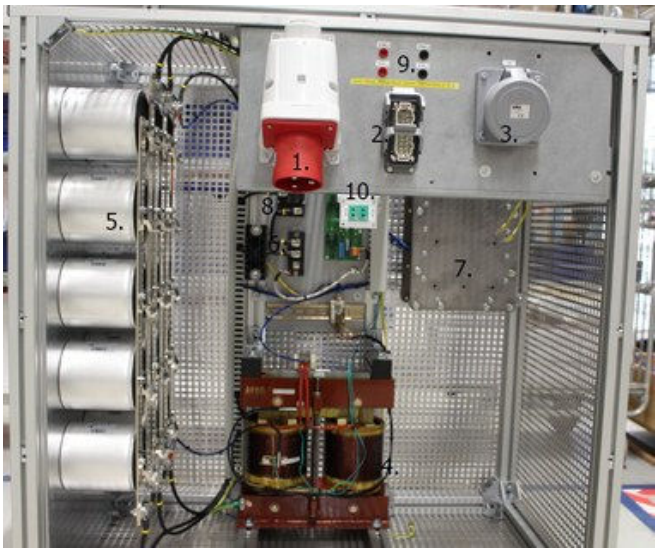


Figure 5.5 — DC Link Cabinet photo

FOCS Cabinet (Fibre Optic Current Sensor) — Exploits the Faraday magneto-optic effect (polarisation rotation proportional to the current). Being all-photonic and air-core, it is inherently immune to the ITER stray field. Its output is the primary closed-loop current feedback to the controller.



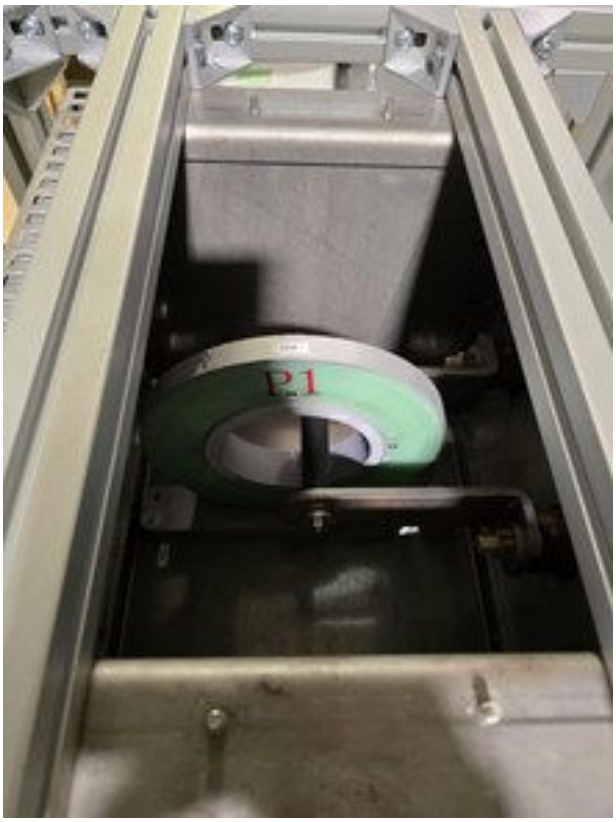


Figure 5.6 — FOCS Cabinet

IGBT Inverter Cabinet — H-bridge output power stage using unipolar PWM with a defined deadtime. Disconnection of its bipolar crowbar was recommended in FAT, since the stored load energy was insufficient to justify the risk of EMI-induced false triggering.



Figure 5.7 — IGBT Inverter Cabinet photo

Load Cabinet — Simulates the ELM coil using parallel resistors and an air-core inductor. Cooling fans keep the enclosure temperature moderate despite high resistor hot-spot temperatures at rated current.



Figure 5.8 — Load Cabinet photo (bottom)

5.2.2 Control System

The PEA is governed by a layered real-time control hierarchy: an operator HMI for setpoints and monitoring; a CPU layer running the operating state machine and the closed-loop PI current controller; an FPGA layer handling PWM generation, thyristor firing, fast protection trips, and current-sensor acquisition; and a physical I/O layer connecting to all cabinets. The PI controller uses FOCS feedback to adjust the IGBT PWM duty cycle every switching period.



Figure 5.9 — Real-time controller in the line filter and control cabinet during SAT. The HMI connects via Ethernet; the FPGA board handles time-critical gate drive and I/O at hardware speed.

5.3 Site Acceptance Test (SAT)

SAT was conducted at the ITER site over approximately one month (29 April to 29 May 2026), following the site commissioning plan and concept of operation under the guidance of the host supervisor. A staged energisation protocol was applied throughout, and all activities complied with the host organisation’s electrical safety procedures.



Figure 5.10 — Electrical safety practice at the ITER site: PPE and safety briefing before SAT activities

5.3.1 Delivery and Mechanical Inspection

29 April 2026 — All seven cabinets were received at the ITER site from the supplier following successful factory acceptance. Visual inspection confirmed no transport damage and cabinet weights consistent with factory records. All cabinets were moved to the SAT test area.



Figure 5.11 — PEA cabinets transported to the SAT test area at the ITER site, 29 April 2026



Figure 5.12 — Cabinet positioned and ready for mechanical inspection at the ITER SAT area

5.3.2 Cable Interconnection

1–3 May 2026 — Power supply cables, earthing/bonding cables, signal harness, and auxiliary supply rails were installed per the connection diagram. One terminal labelling discrepancy was found and corrected before energisation. Checklist signed off. PASS.

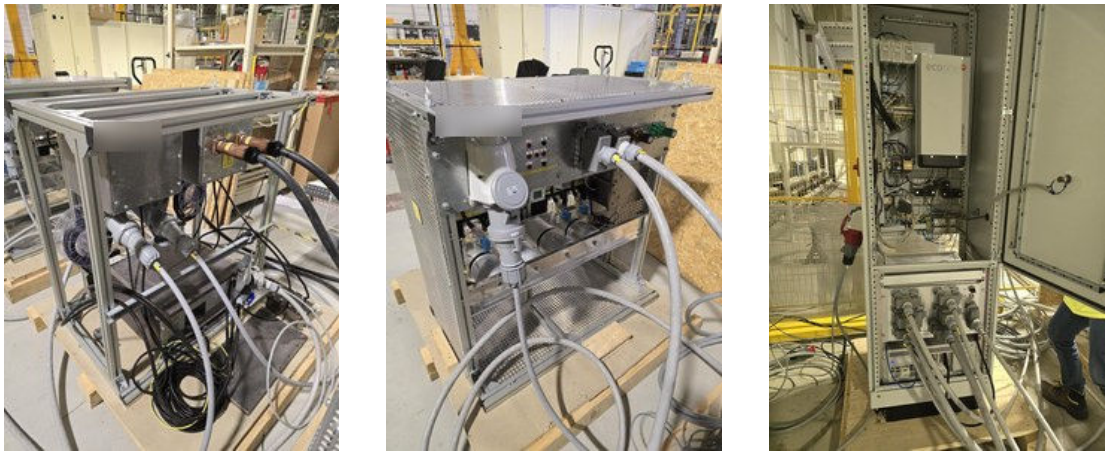


Figure 5.13 — Cable interconnection activities (1–3 May 2026): power busbar routing and signal harness installation between cabinets

5.3.3 First Power-Up

4 May 2026 — Following completion of the required safety checks, the three-phase supply was applied to the line filter and control cabinet. The real-time controller booted into its safe state. Control power rails, digital inputs, HMI communication, and safety interlocks were verified. No spurious alarms or trips. PASS.



Figure 5.14 — First power-up (4 May 2026): HMI active and control system communicating after initial energisation

5.3.4 No-Load Test

With the DC link de-energised, IGBT gate-drive waveforms were measured for all inverter modules. Verified: gate-drive levels, deadtime, absence of shoot-through, correct rise/fall times, and fast-trip response. The DC-link voltage channel and discharge contactors were also verified. PASS.

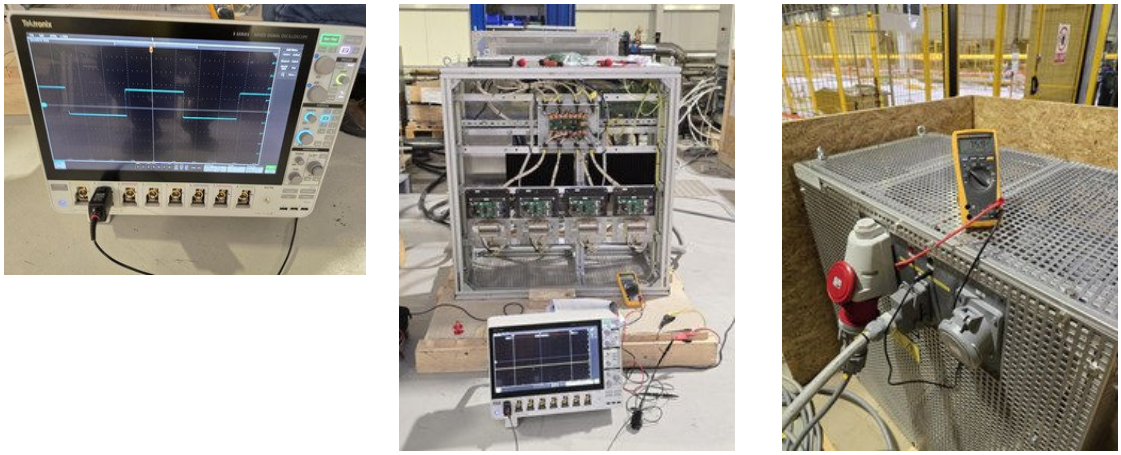


Figure 5.15 — No-Load Test: oscilloscope captures of IGBT gate-drive waveforms confirming gate-drive levels, deadtime, and absence of shoot-through events

5.3.5 Light Load Test

A reduced voltage and low current setpoint were applied to exercise the complete two-stage chain under closed-loop control for the first time on site. Thyristor firing, DC-link charging, IGBT PWM operation, FOCS-based current tracking, output ripple, and thermal behaviour were verified. PASS.

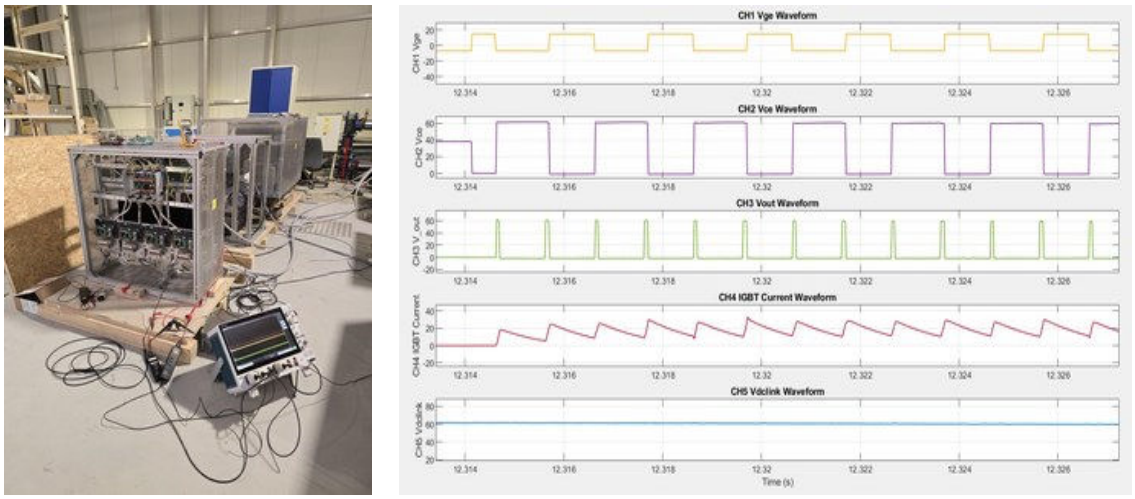


Figure 5.16 — Light Load Test: test activity (left) and output current waveform (right) confirming stable closed-loop current tracking at reduced setpoint

5.3.6 Normal Operation Test — 1-Hour Run

A continuous 60-minute rated-current run was performed. Key results: current tracking stable throughout (no oscillations or resets); IGBT heatsink temperature reached equilibrium; DC-link voltage stable; high power factor; output ripple well below the acceptance criterion. No spurious trips. PASS.

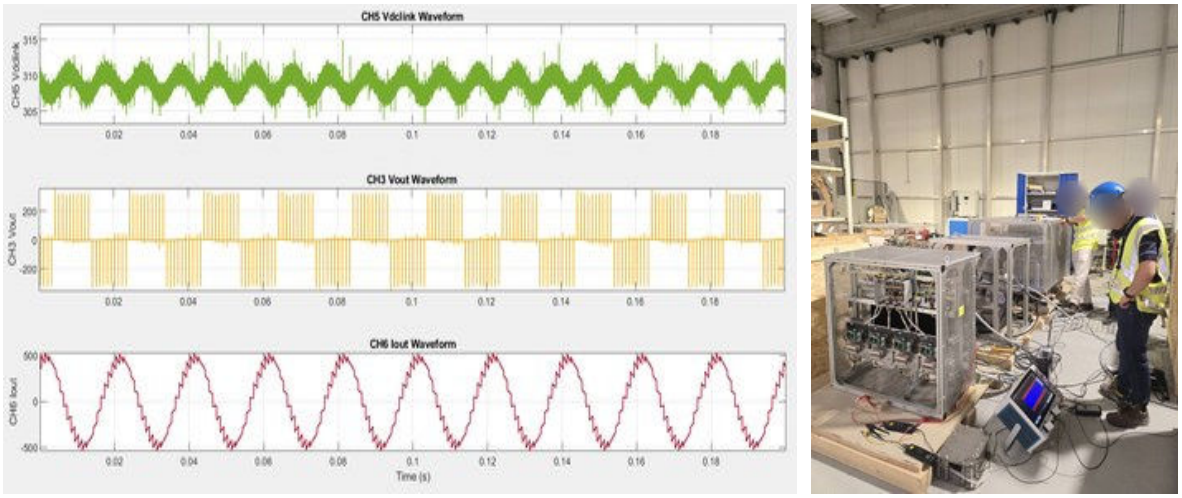


Figure 5.17 — Normal Operation Test: 1-hour rated current waveform trace (left) and test team monitoring the system (right). Both current and DC-link voltage remain stable throughout.

5.3.7 Thermovision Monitoring

Infrared thermovision was conducted concurrently with the 1-hour run. Key findings (consistent with FAT): the load resistors showed the highest temperatures; the IGBT heatsinks showed uniform heat distribution with no hot spots; the thyristor bridge showed very low temperature rise; and all external surfaces remained within touch-safety limits. The PEA was formally declared ready for the SMF qualification campaign.



Figure 5.18 — Thermovision: IR scans of IGBT heatsinks (left) confirming uniform heat distribution; temperature/FOCS monitoring (right)

SAT Phase	Date	Test Description	Result
5.3.1 Delivery & Inspection	29 Apr 2026	Visual inspection; weight/dimension check; no transport damage	PASS
5.3.2 Cable Interconnection	1–3 May 2026	Power, earth, signal, aux cables; connector check; terminal fix	PASS
5.3.3 First Power-Up	4 May 2026	Supply applied; controller boot; control rails; safe mode	PASS
5.3.4 No-Load Test	5–6 May 2026	Gate-drive levels; deadtime; no shoot-through; DC-link measurement	PASS
5.3.5 Light Load Test	7–9 May 2026	Reduced V/I; closed-loop tracking; output ripple; thyristor firing	PASS
5.3.6 Normal Operation (1-hr)	12–15 May 2026	1-hour rated current; stability; thermal behaviour; power factor; ripple	PASS
5.3.7 Thermovision	May 2026	IR scan of inverter and load; heatsink and panel temperature; uniform distribution	PASS

Table 5.1 — SAT test sequence summary: all seven phases PASS

6. Current Sensor SMF Compatibility Test

6.1 Background and Motivation

The ITER tokamak building contains residual Static Magnetic Fields (SMF) well above the threshold that saturates conventional Hall-effect-based current transducers. Because the PEA current measurement chain must remain accurate inside the building, the team conducted qualification tests of a commercial Hall-effect closed-loop current transducer (±1000 A class) to determine whether it could serve as a secondary or backup sensor alongside the primary FOCS.

The FOCS is immune to SMF by design (Faraday magneto-optic effect, air-core). However, any supplementary diagnostic or calibration sensor must also pass SMF qualification. These tests were performed under two ITER test protocols.

6.2 Test Setup and Methodology

6.2.1 Sensor Under Test

The sensor under test is a Hall-effect closed-loop (flux-compensated) transducer. Its closed-loop topology suppresses some interference, but the Hall element is inherently susceptible to external DC magnetic fields. The criterion adopted for ITER acceptance was a measurement error of no more than ±10 A across all SMF conditions.

6.2.2 Test Configurations

Both protocols applied a controlled external SMF in stepped increments (0 → 50 mT → 70 mT → 0) using a permanent magnet assembly while a known DC primary current (1000 A from a current source) was injected, comparing the sensor output against a reference. The first protocol tested four mounting configurations (Test 1 to Test 4, T1–T4) by varying sensor orientation relative to the field direction, while the second repeated the test across six field directions. The acceptance criterion was defined by the maximum allowable error specified in the sensor manufacturer's manual.

6.2.3 Test Results

Pre-test baseline: With no SMF and operating at rated current, sensor output met the baseline criteria. All four configurations were confirmed to be within specification prior to SMF exposure.

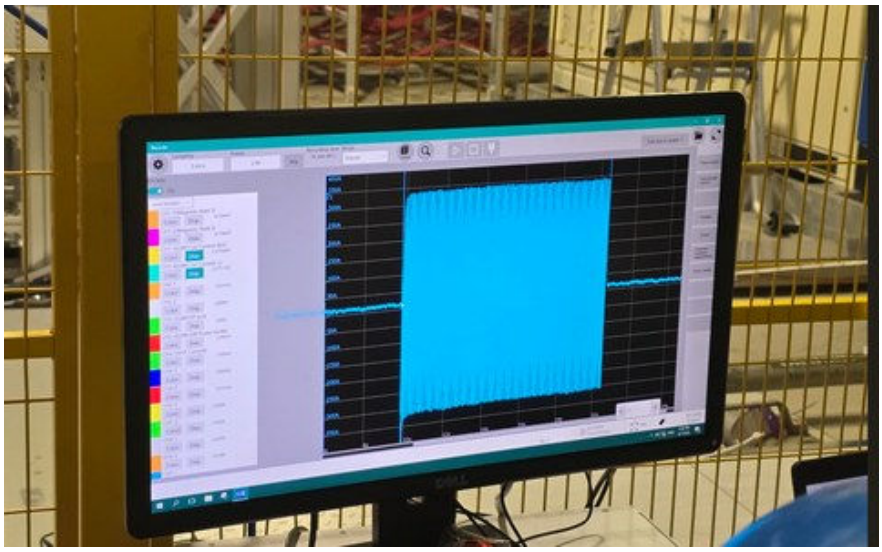


Figure 6.1 — Pre-test baseline: sensor output at rated 1000 A with no applied SMF, all four configurations within ±1 A (reference).

6.2.3.1 Test T1 — Cable Installed + 100 A Injected

Configuration: Primary cable (~100 A RMS AC) routed through sensor aperture. SMF applied 0 → 50 → 70 mT.

Expected: Calc ≈ 100 A steady, independent of B-field.

Observed: Sensor output rises directly with B-field: ~+162 A at 50 mT, ~+224 A at 70 mT. The field-induced offset completely masks the real 100 A signal.



Figure 6.2 — T1: Test setup — primary cable (~100 A RMS AC) routed through the sensor aperture.

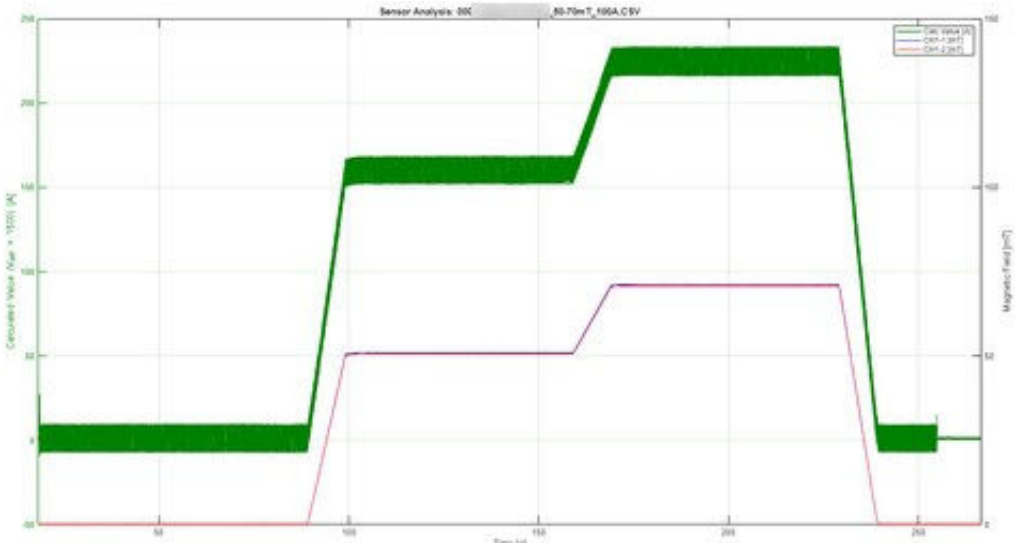


Figure 6.3 — T1: Calculated current (green, left axis) vs. B-field (right axis). Output tracks SMF steps rather than the 100 A primary current.

6.2.3.2 Test T2 — Cable Installed, No Current

Configuration: Cable present in aperture, no current injected. SMF applied 0 → 50 → 70 mT.

Expected: Calc ≈ 0 A (flat line — no current flowing).

Observed: Calc rises to ~+161 A at 50 mT and ~+225 A at 70 mT with zero real current. Confirms that SMF alone — not the cable current — is the source of the error.



Figure 6.4 — T2: Test setup — cable still installed in the sensor aperture with no current injected (same physical configuration as T1).

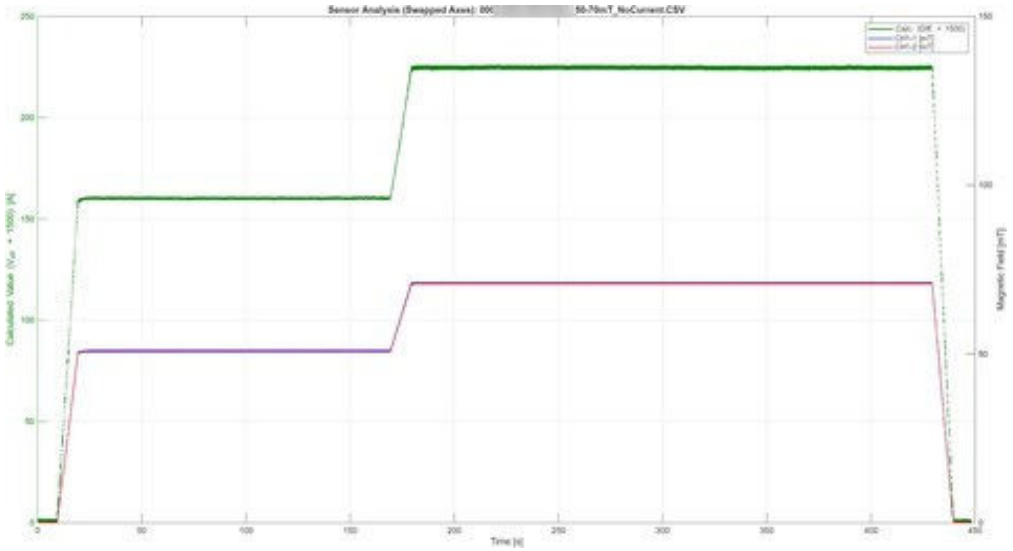


Figure 6.5 — T2: With no current injected, the sensor output mirrors the B-field steps identically.

6.2.3.3 Test T3 — No Cable, Standard Orientation

Configuration: Cable removed entirely. Sensor installed in standard orientation. SMF applied 0 → 50 → 70 mT.

Expected: Calc ≈ 0 A (no cable, no current).

Observed: Same error pattern persists: ~+162 A at 50 mT, ~+223 A at 70 mT. The sensor core itself is intrinsically susceptible to the external field.



Figure 6.6 — T3: Test setup — sensor with the primary cable removed, standard orientation.

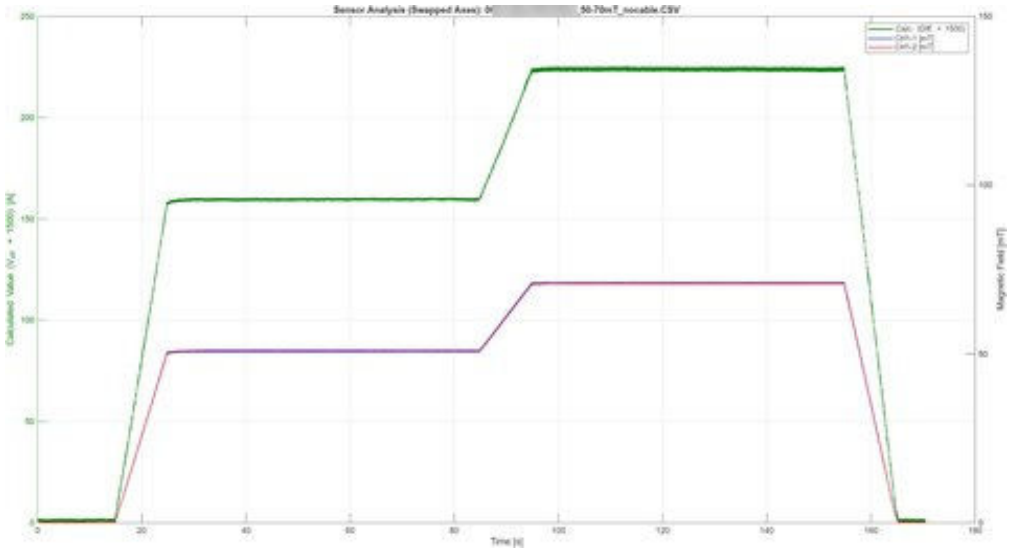


Figure 6.7 — T3: Even without a cable, calculated current closely tracks the B-field — confirming intrinsic sensor susceptibility.

6.2.3.4 Test T4 — No Cable, Sensor Rotated 90°

Configuration: Cable removed. Sensor rotated 90° relative to dominant field direction. SMF applied 0 → 50 → 70 mT.

Expected: Reduced coupling if orientation matters (error < ±10 A).

Observed: Error is significantly reduced (−12 to −16 A) compared to standard orientation but still exceeds the ±10 A specification limit. High noise ripple and transient spikes (±50 A) observed at field transitions.

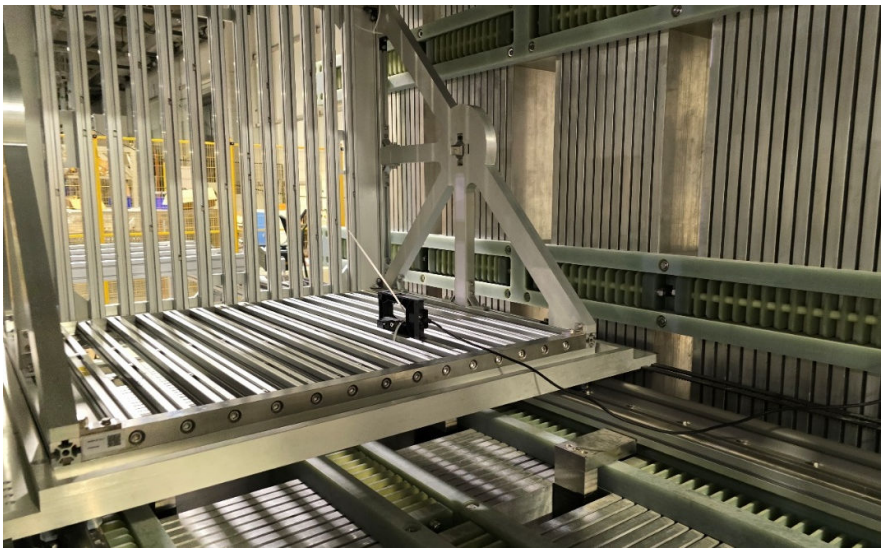


Figure 6.8 — T4: Test setup — sensor with cable removed, rotated 90° relative to the dominant field direction.

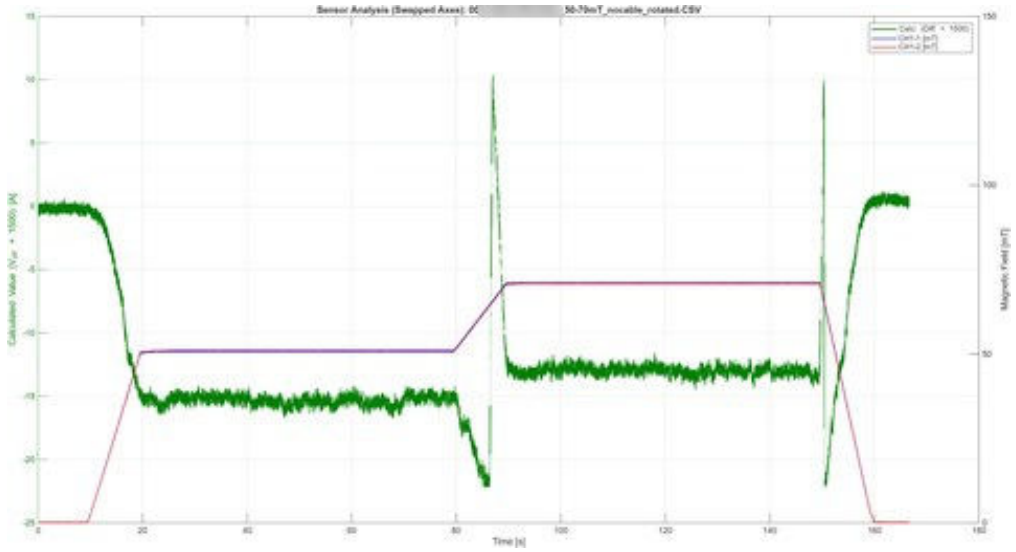


Figure 6.9 — T4: Rotated 90° — error reduces to ~−13 to −16 A but remains outside specification. Note high noise at field step transitions.

6.3 Conclusions from SMF Test

The tested current transducer fails to maintain its ±10 A accuracy specification under all tested SMF conditions at 50 mT and 70 mT. In standard orientation, the external field induces an erroneous DC offset of +161 A to +224 A approximately 16 to 22 times the allowable limit. Rotating the sensor 90° reduces the error to −12 to −16 A, which still marginally exceeds the specification. The error is present even when no cable or current is applied, confirming that the sensor core itself is intrinsically coupled to the external field. The tested current transducer is not suitable for use in environments with static magnetic fields ≥ 50 mT without additional mitigation.

Test	Configuration	B-Field (mT)	Sensor Output (A)	True Current (A)	Error (A)	Result
T1	100 A + Cable, standard	~51 mT	+162	~0 (DC avg)	**+162**	**FAIL**
		~71 mT	+224	~0 (DC avg)	**+224**	**FAIL**
T2	No current, cable installed	~50 mT	+161	0	**+161**	**FAIL**
		~70 mT	+225	0	**+225**	**FAIL**
T3	No current, no cable, standard	~50 mT	+162	0	**+162**	**FAIL**
		~70 mT	+223	0	**+223**	**FAIL**
T4	No current, no cable, rotated 90°	~50 mT	−15.6	0	**−15.6**	**FAIL**
		~70 mT	−12.3	0	**−12.3**	**FAIL**

Table 6.1 — SMF test summary: tested Hall-effect sensor disqualified for SMF Test (±10 A criterion)

Recommendations

- Retest with Busbar: Conduct future tests using a rigid busbar to minimize geometry-related errors.
- Retest with Magnetic Shielding: Enclose the unit in a mu-metal shield to attenuate external fields.
- Alternative Technology: Evaluate Fiber Optic Current Sensors (FOCS) for testing, as they are inherently immune to magnetic fields.

7. Conclusions

This two-month visiting research programme (1 April – 29 May 2026) at the ITER Organization provided immersive, hands-on engagement with the complete Power Electronics Assembly system — from factory acceptance testing through site commissioning and instrument qualification.

7.1 Technical Achievements

The following technical objectives were met during the placement:

- SAT Completion: All seven SAT phases (delivery inspection, cable interconnection, first power-up, no-load, light load, normal operation 1-hour run, thermovision) were successfully completed with PASS results for every test item.
- System Performance Validated: The PEA prototype demonstrated stable closed-loop current tracking at rated current over 1-hour, stable DC-link voltage, and thermal margins well within design limits.
- SMF Qualification: The tested Hall-effect sensor was conclusively shown to be incompatible with the SMF environment of the ITER tokamak building (errors up to +225 A vs. ±10 A criterion). This result highlights the necessity for proper re-testing or deploying an alternative sensor to prevent the installation of an unreliable device.
- FAT Review: The factory acceptance test documentation was reviewed in depth, enabling thorough preparation for SAT activities and an understanding of the design basis for each test criterion.
- Technical Documentation: Prepared written summaries of the SMF test protocols and results; contributed to SAT checklist closure documentation.

7.2 Key Lessons

Several engineering insights emerged from direct observation and participation:

- Physics-driven sensor selection: The SMF environment at ITER is not an edge case — it is the normal operating condition. Any instrument placed inside the tokamak building must be validated against the full stray field spectrum, not just near-zero-field specifications. FOCS technology is not merely preferred; it is necessary.
- Staged commissioning discipline: The controller's staged operating states and the staged energisation protocol (no-load before light-load before rated) are not procedural formalities. They systematically isolate failure modes, preventing cascading damage to high-value components.
- Importance of a FAT baseline: The rigorously documented FAT compressed SAT preparation time significantly. Every test in the SAT had a direct FAT counterpart, with acceptance criteria already agreed and traceable.
- Cross-disciplinary integration: Safe high-power electronics commissioning at a nuclear facility requires simultaneously mastering power electronics, Functional Safety, radiation/EMC environments, and institutional ITER safety protocols — an integration that is difficult to replicate in a conventional power plant environment.

8. Professional Development

8.1 Technical Skills Gained

Direct participation in SAT activities and SMF testing delivered measurable growth across several technical domains:

- Power electronics: thyristor phase control, IGBT H-bridge operation, unipolar PWM — experienced on live high-current equipment rather than in simulation.
- Magneto-optic sensing: operational understanding of the Faraday-effect FOCS
- High-power commissioning: staged energisation, formal work-authorisation and isolation procedures, and arc-flash protective requirements.
- Real-time control: layered real-time control hierarchy; FPGA-layer gate-drive timing; PI current control loop tuning philosophy.
- Test documentation: FAT/SAT report structure, non-conformance reporting workflow, and formal document management practice.

8.2 Institutional and Cultural Knowledge

ITER is the most complex collaborative engineering project in operation today — seven Members representing 34 participating nations, multiple Domestic Agencies, a resident staff, and a construction site hosting hundreds of contractors simultaneously. Embedded participation revealed:

- How large-scale international contracts are structured (IO as client, domestic agencies as suppliers, industrial contractors under domestic agencies).
- The role of the ITER document management system (IDM) as the authoritative source for all design, test, and approval records — and the discipline required to maintain traceable version control.
- Multi-cultural technical collaboration: daily interactions with colleagues from France, China, Sweden, Korea, India, and the EU working under a common technical vocabulary.

9. References

[1] ITER Organization, "Facts & Figures." [Online]. Available: iter.org/facts-figures. Accessed: June 2026.

[2] ITER Organization, "In a Few Lines." [Online]. Available: iter.org/few-lines. Accessed: June 2026.

[3] ITER Organization, "ITER Goals." [Online]. Available: iter.org/fusion-energy/what-will-iter-do. Accessed: June 2026.

[4] ITER Organization, "Magnets." [Online]. Available: iter.org/machine/magnets. Accessed: June 2026.

[5] ITER Organization, "Making Fusion Work." [Online]. Available: iter.org/fusion-energy/making-it-work. Accessed: June 2026.

[6] ITER Organization, "The ITER Tokamak." [Online]. Available: iter.org/machine. Accessed: June 2026.

[7] ITER Organization, "Vacuum Vessel." [Online]. Available: iter.org/machine/vacuum-vessel.

[8] ITER Organization, "What is a Tokamak?" [Online]. Available: iter.org/machine/what-tokamak.

[9] S. Wang, G. Gao, Z. Sheng, Y. Yang, and L. Wang, "Analysis and test of a 1m / 275 mT large-scale high-intensity magnetic field immunity test coil system for ITER," *Fusion Engineering and Design*, 2023.

[10] S. Wang, G. Gao, Z. Sheng, et al., "Final design of the static magnetic field test facility for the ITER tokamak devices," *Fusion Engineering and Design*, 2023.